

Antiferromagnetic resonance in the canted phase of $\text{La}_{1-x}\text{Sr}_x\text{MnO}_3$: Experimental evidence against electronic phase separation

A. A. MUKHIN¹, V. YU. IVANOV¹, V. D. TRAVKIN¹, A. PIMENOV²,
A. LOIDL² and A. M. BALBASHOV³

¹ *General Physics Institute of the Russian Academy of Sciences
38 Vavilov St., 117942 Moscow, Russia*

² *Experimentalphysik V, EKM, Universität Augsburg - 86135 Augsburg, Germany*

³ *Moscow Power Engineering Institute*

14 Krasnokazarmennaya St., 105835 Moscow, Russia

Abstract. – Antiferromagnetic resonance (AFMR) experiments were performed in $\text{La}_{1-x}\text{Sr}_x\text{MnO}_3$ single crystals for Sr concentrations $0 \leq x \leq 0.1$. A quasi-optical technique was employed in a frequency range $2 \text{ cm}^{-1} < \nu < 30 \text{ cm}^{-1}$ and for temperatures $3 \text{ K} < T < 300 \text{ K}$. Two AFMR modes, a quasi-ferromagnetic (F) and a quasi-antiferromagnetic (AF) mode, were observed for temperatures below T_N . The resonance frequency of the F-mode reveals a strong concentration dependence, while the AF-mode frequency only slightly decreases on increasing x . The observed concentration dependencies, as well as the excitation conditions for both modes, can be explained using a simple two-sublattice model. These experiments provide direct evidence in favour of a canted antiferromagnetic (CA) structure for $x < 0.1$ and low temperatures and cannot be interpreted in terms of a phase separation of ferromagnetic droplets in an antiferromagnetic matrix.

Introduction. – The observation of the colossal negative magnetoresistance in doped manganites $\text{R}_{1-x}\text{A}_x\text{MnO}_3$, where R is a trivalent rare-earth ion and A is a divalent ion, such as Ca or Sr, has attracted considerable interest [1]. The parent compound LaMnO_3 reveals a Jahn-Teller distorted orthorhombic crystal structure and is ordered antiferromagnetically below $T_N \approx 140 \text{ K}$ [2, 3]. The manganese ions, Mn^{3+} , exhibit a $3d^4$ electronic configuration with a total spin $S = 2$, where three electrons occupy the t_{2g} orbitals with a local spin of $S = 3/2$, while the remaining electron occupies an e_g orbital hybridized with the oxygen $2p$ states. The spins of the t_{2g} and e_g electrons are aligned parallel to each other due to double exchange coupling. Due to the co-operative Jahn-Teller effect the e_g orbitals of the Mn^{3+} ions are ordered below $T = 780 \text{ K}$ resulting in an antiferromagnetic layered spin structure with the Mn^{3+} spins ferromagnetically coupled in the basal ab -plane and antiferromagnetically coupled along the c -axis [3].

The substitution of divalent ions (Sr or Ca) results in doping of holes into the e_g orbitals and allows hopping of e_g electrons from a Mn^{3+} ion to neighbouring holes at a Mn^{4+} site, which induces the ferromagnetic interaction between Mn ions due to the on-site Hund's rule coupling. This transition from a (canted) antiferromagnetic and insulating to a ferromagnetic

metallic state occurs for the concentrations $x > 0.15$ and has been described within a double-exchange mechanism by Zener [4]. A theoretical analysis of the double exchange effects in the doped manganites was carried out by de Gennes [5], who predicted an evolution of the magnetic structure from the antiferromagnetic state to the ferromagnetic one via a canted (CA) phase and an existence of two branches in the spin wave spectra [5].

The possibility of phase separation into AFM and FM domains was pointed out early by Wollan and Koehler [3] and the possible instability of a canted phase against electronic phase separation was discussed by Nagaev [6] and Khomskii and Sawatzky [7]. New alternative models were developed recently [8, 9], which favour an electronic phase separation into hole-poor antiferromagnetic and hole-rich ferromagnetic regions and predict an instability of the CA magnetic structure of manganites. However, it was not clear, which approach is more applicable for these compounds as a majority of experimental data could be explained within both models, *i.e.* by the canted structure and by an electronic phase separation. As the spin excitation spectra are sensitive to the magnetic structure they may provide a key information to clarify this situation.

Magnetic resonance offers a powerful tool to study the interactions in a coupled spin system. The main aspects of the theory of magnetic resonance have been established more than thirty years ago [10, 11]. The characteristic frequencies of AFMR-modes for most antiferromagnetically ordered substances lie in the range between infrared and microwaves [12]. Recent inelastic-neutron-scattering (INS) experiments revealed spin excitations in pure LaMnO_3 [13], which are consistent with the antiferromagnetic layered structure ($A_y F_z$). These data showed a gap of about 20 cm^{-1} at low temperatures and a strong anisotropy of the dispersion along and perpendicular to the c -axis [13]. This value agrees well with the AFMR frequency in pure LaMnO_3 that was found to be $\sim 18 \text{ cm}^{-1}$ at zero magnetic field and at low temperatures [14]. The behaviour of AFMR frequencies in an external magnetic field could be well explained using a two-sublattice model [15]. This model results in a canted magnetic structure through the Dzyaloshinsky-Moriya (D-M) interaction [11, 16] and the single ion anisotropy [11]. The preliminary submillimeter-wave data on Sr-doped LaMnO_3 showed that the AFMR line even in the parent compound is splitted into two lines with frequencies of about 18.1 and 17.3 cm^{-1} at 4.2 K [17]. This splitting strongly increases with Sr-doping and two well-separated modes could be observed for $\text{La}_{0.95}\text{Sr}_{0.05}\text{MnO}_3$ which had different excitation conditions. The change of the spin-wave frequencies upon doping may be compared with similar observation in Ca-doped LaMnO_3 [18].

In order to study the transformation of the spin-wave spectra with hole doping in more detail, we performed a systematic investigation of antiferromagnetic resonances in weakly doped $\text{La}_{1-x}\text{Sr}_x\text{MnO}_3$ for a set of Sr concentrations $0 < x < 0.1$ and in the submillimeter frequency range $2 \text{ cm}^{-1} < \nu < 30 \text{ cm}^{-1}$.

Experimental. – Single crystals of $\text{La}_{1-x}\text{Sr}_x\text{MnO}_3$ ($0 \leq x \leq 0.1$) were grown by a floating zone method with radiation heating [19]. X-ray powder diffraction measurements revealed single phase crystals. However, X-ray topography indicated that the samples were twinned except for concentrations $x = 0.025$ and 0.05 . Magnetization $M(T, H)$, ac susceptibility $\chi_{ac}(T)$ and dc-resistivity data for these crystals were published elsewhere [20]. Transmission $T(\nu)$ spectra of thin plane-parallel plates with a thickness $d \sim 1 \text{ mm}$ were measured in the frequency range $2 \text{ cm}^{-1} < \nu < 30 \text{ cm}^{-1}$ by means of a quasi-optical backward-wave-oscillator technique [21] at temperatures $3 \text{ K} < T < 300 \text{ K}$.

Results and discussion. – Figure 1 shows examples of the $T(\nu)$ spectra for different concentrations and at low temperatures. A common feature of these spectra is the existence of periodic oscillations due to the interference of a radiation inside a plane-parallel plate. On

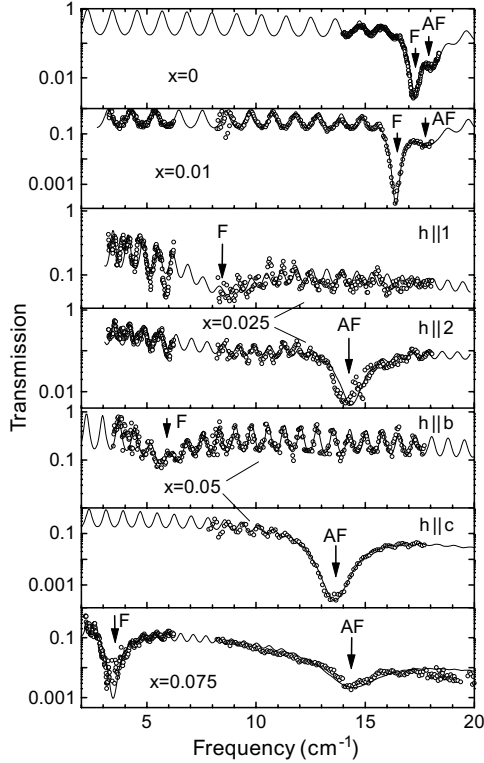


Fig. 1

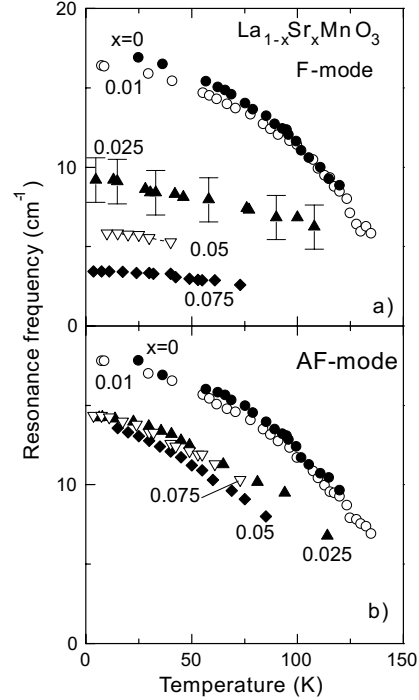


Fig. 2

Fig. 1 – Low-temperature transmission spectra of $\text{La}_{1-x}\text{Sr}_x\text{MnO}_3$ at different concentrations. Arrows indicate the positions of the F- and AF-modes, points are the experiment, solid lines are based on the Fresnel equations and eq. (1).

Fig. 2 – Temperature dependence of the resonance frequencies of the F (a) and AF (b) modes in $\text{La}_{1-x}\text{Sr}_x\text{MnO}_3$ for different concentrations.

the background of these oscillations pronounced absorption lines were observed below the Néel temperatures, which can be identified as two AFMR modes, a quasi-ferromagnetic (F) and a quasi-antiferromagnetic (AF) one. In twinned samples both modes were observed simultaneously in the same polarization of the alternating field (h) for $x = 0, 0.01, 0.075$ despite a strong difference of their excitation conditions: $h||a$ -, b -axes for the F-mode and $h||c$ -axis for the AF-mode [17]. The only composition which practically did not contain twins was the $\text{La}_{0.95}\text{Sr}_{0.05}\text{MnO}_3$ sample, for which the F-mode was excited for $h||b$ and the AF-mode for $h||c$, in excellent agreement with the excitation conditions for a layered A_yF_z structure. We also note the polarization sensitivity of the spectra for $x = 0.025$, where the F- and AF-modes were observed separately for two perpendicular ($h||1$ and $h||2$) polarizations. However, the identification of crystallographic axes in this sample was not possible.

In order to determine the frequency and the strength of these modes we have fitted the $T(\nu)$ spectra using Fresnel's formulas for the transmission of the plane-parallel plate and a harmonic oscillator model for the permeability dispersion:

$$\mu(\nu) = 1 + \sum_k \frac{\Delta\mu_k \nu_k^2}{(\nu_k^2 - \nu^2 + i\nu\Delta\nu_k)}; \quad (1)$$

here ν_k , $\Delta\nu_k$ and $\Delta\mu_k$ are the resonance frequency, the linewidth and the mode contribution to the static permeability of the k -th mode, respectively. The results of these fits are indicated

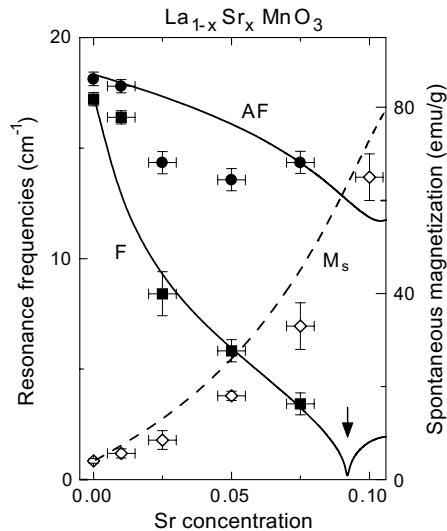


Fig. 3

Fig. 3 – Concentration dependence of the low-temperature resonance frequencies of the F- and AF-modes (left scale) and spontaneous magnetization (right scale). Symbols: experiment, lines: theory. The arrow indicates the predicted position of the spin reorientation transition $A_yF_z-A_zF_y$.

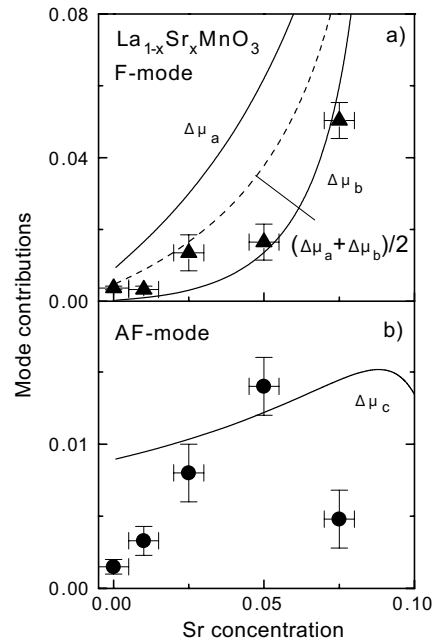


Fig. 4

Fig. 4 – Concentration dependence of the F (a) and AF (b) mode contributions in $\text{La}_{1-x}\text{Sr}_x\text{MnO}_3$. Points are obtained from the fits to the transmission coefficient (fig. 1); solid lines: theory (eqs. (6)-(8)).

as solid lines in fig. 1. The temperature dependences of the F- and AF-mode frequencies are presented in fig. 2 for different hole concentrations x .

Figure 3 shows the concentration dependence of both AFMR-mode frequencies for low temperatures ($T < 20\text{K}$). The resonance frequency of the F-mode (full squares) strongly decreases with increasing Sr concentration while the resonance frequency of the AF-mode (full circles) depends only weakly on x . In addition, fig. 3 represents the concentration dependence of the spontaneous magnetization (open rhombs) which obviously correlates with the decrease of the F-mode frequency.

Finally, the strengths of the AFMR modes are indicated in fig. 4 as a function of Sr concentration. The mode contribution to the F-mode (fig. 4a, full triangles) steadily increases with increasing doping x . The AF-mode contribution (fig. 4b, full circles) passes through a maximum close to $x = 0.05$.

We have adopted a simple two sublattice model to describe the canted magnetic structure and the observed AFMR. In this case the free energy of the system coincides with that of the Gennes free-carrier model [5]. For a realistic description, in addition to the free energy also contributions of the single ion anisotropy, $D_x \sum_i S_{xi}^2 + D_z \sum_i S_{zi}^2$, and antisymmetric exchange interactions $(D - M)$, $\sum_{i,j} \mathbf{d}_{ij}[\mathbf{S}_i \mathbf{S}_j]$, have to be taken into account. In this limit the free energy at $T = 0$ is given by

$$F(\mathbf{m}, \mathbf{l}) = \frac{1}{2} A m^2 - B |\mathbf{m}| + \frac{1}{2} K_x (m_x^2 + l_x^2) + \frac{1}{2} K_z (m_z^2 + l_z^2) - d(m_z l_y - m_y l_z) - M_0 \mathbf{m} \mathbf{H}. \quad (2)$$

The first and the second terms describe antiferromagnetic and ferromagnetic (double) exchange, respectively, the third and fourth terms give the single ion anisotropy, the fifth term describes the antisymmetric Dzialoshinski-Moriya exchange and the last term gives the effect of an external magnetic field. In eq. (2) \mathbf{m} and \mathbf{l} are the dimensionless ferro- and antiferromagnetic vectors, which are defined as $\mathbf{m} = (\vec{M}_1 + \vec{M}_2)/2M_0$, $\mathbf{l} = (\vec{M}_1 - \vec{M}_2)/2M_0$ and satisfy the conditions $\mathbf{m}\mathbf{l} = 0$, $\mathbf{m}^2 + \mathbf{l}^2 = 1$ since the sublattices \vec{M}_1 and \vec{M}_2 are assumed to be saturated at $T = 0$. $A = -2NzJ_{\parallel}S^2(1 - \alpha x)$ describes the effective interlayer antiferromagnetic exchange constant. $B = xNzt_{\parallel}/2 \equiv \beta x$ is the double-exchange constant which is determined by the transfer integral t_{\parallel} of the e_g electrons along the c -axis. $K_{x,z} = ND_{x,z}S^2(1 - x) > 0$ are anisotropy constants stabilizing the A_yF_z configuration in pure LaMnO_3 . $d = Nd_{\parallel}S^2z(1 - x)$ is the interlayer antisymmetric exchange constant. $M_0 = (1 - x)M_0(\text{Mn}^{3+}) + xM_0(\text{Mn}^{4+})$ is the saturation magnetization of the sublattices. $z = 2$ is the number of the nearest Mn neighbours along the c -axis and N is the total number of the Mn ions in the crystal. Further, we have introduced a linear concentration dependence of K_x , K_z and d , which is determined by the concentration of Mn^{3+} ions, and we have taken into account the phenomenological concentration dependence of the exchange constant $A \sim (1 - \alpha x)$ due to a possible change of the orbital structure and other mechanisms.

The equilibrium amplitudes of \mathbf{m} and \mathbf{l} were determined from the minimum of the free energy and can be expressed as: $m_z = \cos(\theta/2)$ and $l_y = \sin(\theta/2)$, where θ is the angle between the sublattice magnetizations, given by the equation:

$$\cos(\theta/2) = [B + M_0H_z + d \sin(\theta/2)]/[A + K_z + d \text{ctg}(\theta/2)]. \quad (3)$$

Using the dynamic equations of motion and neglecting dissipation terms, the components of the dynamic magnetic susceptibility, $\chi_{xx,yy}(\omega) = \Delta\chi_{xx,yy}\omega_F^2/(\omega_F^2 - \omega^2)$ and $\chi_{zz}(\omega) = \Delta\chi_{zz}\omega_{AF}^2/(\omega_{AF}^2 - \omega^2)$ were calculated. The resonance frequencies of the F (ω_F) and AF (ω_{AF}) modes and the corresponding mode contributions to the static magnetic susceptibility $\Delta\chi_{kk}$ are given by

$$(M_0\omega_F/\gamma)^2 = [M_0H_z \cos(\theta/2) - K_z \cos \theta][M_0H_z + d \sin(\theta/2) + (K_x - K_z) \cos(\theta/2)]/\cos(\theta/2), \quad (4)$$

$$(M_0\omega_{AF}/\gamma)^2 = [K_x \sin(\theta/2) + d \cos(\theta/2)][(A + K_z) \sin(\theta/2) + d \cos(\theta/2)(3 + \text{ctg}^2(\theta/2))], \quad (5)$$

$$\Delta\chi_{xx} = M_0^2 \cos(\theta/2)/[M_0H_z + d \sin(\theta/2) + (K_x - K_z) \cos(\theta/2)], \quad (6)$$

$$\Delta\chi_{yy} = M_0^2 \cos^2(\theta/2)/[(-K_z) \cos \theta + M_0H_z \cos(\theta/2)], \quad (7)$$

$$\Delta\chi_{zz} = M_0^2/[(A + K_z) + d \text{ctg}(\theta/2)(3 + \text{ctg}^2(\theta/2))], \quad (8)$$

where $\gamma = g\mu_B/\hbar$, $g \approx 2$.

The concentration dependencies of the AFMR frequencies, the mode contributions to the static permeability $\Delta\mu_k = 4\pi\Delta\chi_{kk}$ and the spontaneous magnetization $M_S = M_0 \cos(\theta/2)$ for $T = 0$ and $H_z = 0$ were calculated and are shown as dashed lines in fig. 3, 4. The main parameters $K_z(x = 0) = 3.9 \cdot 10^6$ erg/g, $K_x(x = 0) = 4.1 \cdot 10^6$ erg/g, $d(x = 0) = 3.3 \cdot 10^6$ erg/g were determined using the data for two AFMR frequencies and the value of spontaneous magnetization in pure LaMnO_3 . The exchange constant $A(x = 0) = 7.3 \cdot 10^7$ erg/g was taken from the neutron scattering data [13] for the interlayer exchange in pure LaMnO_3 . Therefore, only two parameters remain to fit the concentration dependence of the AFMR lines. These two remaining constants β and α were considered as fitting parameters, and were determined as $\beta = 2.43 \cdot 10^8$ erg/g and $\alpha = 6.6$. The calculated dependencies of resonance frequencies (solid lines in fig. 3), mode contributions (lines in fig. 4) and spontaneous magnetization (dashed line in fig. 3) describe the experimental data qualitatively and quantitatively reasonably well. In

particular, the softening of the F-mode, the weak concentration dependence of the AF-mode and the spontaneous magnetization are in qualitative agreement with the model calculations. In the range $0.09 \leq x \leq 0.1$ a spin-reorientation transition, $A_y F_z - A_z F_y$, is predicted, which occurs when $\theta = \pi/2$ and originates from a competition of the m_z^2 and l_z^2 contributions to the anisotropy energy (eq. (2)). The F-mode contribution $\Delta\mu_y$ (eq. (7)) is determined by the rotational susceptibility and diverges at the spin reorientation (fig. 4a). A considerable increase of the F-mode contributions $\Delta\mu_x$ and $\Delta\mu_y$ with increasing Sr concentration is in qualitative agreement with the experiment, however due to the twin structure, the experimental values are systematically smaller than theoretically predicted. The same tendency is also observed in case of the AF-mode contribution $\Delta\mu_z$ (fig. 4b).

The observed softening of the F-mode and its transformation into the ferromagnetic resonance mode (FMR) is in agreement with a recent FMR study of $\text{La}_{0.9}\text{Sr}_{0.1}\text{MnO}_3$ [22], where a FMR at zero magnetic field was observed at a frequency of approximately 0.5 cm^{-1} for $T = 100 \text{ K}$.

Comparison of our data for $\text{La}_{1-x}\text{Sr}_x\text{MnO}_3$ with neutron-scattering experiments on $\text{La}_{1-x}\text{Ca}_x\text{MnO}_3$ [18] shows a qualitative similarity. In both systems two magnetic modes were observed, one of which has a resonance frequency of about 20% lower than in the pure system, while the other mode has a tendency to soften with increasing hole doping. However, in ref. [18] the origin of the low-frequency mode was associated with a new kind of magnetic excitations related to appearance of magnetic inhomogeneities (magnetic droplets or magnetic polarons) while the high-frequency mode was identified with spin waves inherent to pure LaMnO_3 . Our AFMR-data do not confirm this picture for the $\text{La}_{1-x}\text{Sr}_x\text{MnO}_3$ system and suggest the origin of both modes from the canted magnetic structure at low temperatures. This conclusion is strongly supported by the excitation conditions for the observed modes. According to the symmetry considerations for the canted structure and for the platelet sample with the a -axis perpendicular to the plane, the high-frequency AF-mode is excited only for the $h\parallel c$ -axis and the F-mode is excited for the $h\parallel b$ -axis, which in fact was observed for untwinned $\text{La}_{0.95}\text{Sr}_{0.05}\text{MnO}_3$ (fig. 1). According to the scenario proposed in [18], the AF- and F-modes have to be observed close to each other and should be excited both, for the $h\parallel c$ and the $h\perp c$ -axis.

Assuming electronic phase separation of ferromagnetic droplets within an antiferromagnetic matrix, two AFMR modes with frequencies corresponding to the pure LaMnO_3 ($17\text{--}18 \text{ cm}^{-1}$) and one ferromagnetic mode with much lower frequency ($\nu_0 < 4 \text{ cm}^{-1}$) are expected. The AFMR modes have to be excited both by the $h\perp c$ and the $h\parallel c$ -axis. But our data for the untwinned $\text{La}_{0.95}\text{Sr}_{0.05}\text{MnO}_3$ sample clearly demonstrate (fig. 1) that there is only one high-frequency AFMR mode excited by $h\parallel c$ while the second AFMR mode with a slightly different frequency, excited by the $h\perp c$ -axis, does not exist. Moreover, the magnetic field would split the expected two AFMR modes. The preliminary submillimeter-wave measurements in magnetic field up to 7 T, which are now in progress, did not reveal any splitting. Finally, the concentration dependence on the AFMR frequencies, shown in fig. 1 and fig. 2, clearly demonstrates the splitting up of the second mode and its transformation to the ferromagnetic resonance. Therefore the phase separation picture cannot explain the present results.

Conclusions. – In conclusion, we have investigated the concentration dependence of the AFM resonances in $\text{La}_{1-x}\text{Sr}_x\text{MnO}_3$ for $0 < x < 0.1$. The remarkable softening of the quasi-ferromagnetic mode and its transformation to a ferromagnetic resonance mode correlates well with the increase of the spontaneous magnetic moment. The full set of data can be explained using a simple two-sublattice model, which clearly indicates the existence of the canted magnetic structure in weakly doped manganites. We conclude that in $\text{La}_{1-x}\text{Sr}_x\text{MnO}_3$

no electronic phase separation into ferro- and antiferromagnetic droplets or stripes exist for $x < 0.1$.

This work was supported in part by RFBR (Grants No. 99-02-16849 and 97-02-17325), by BMBF via the contract EKM (13N6917/0) and by the European Community via INTAS (97-30850).

REFERENCES

- [1] VON HELMOLT R., WECKER J., HOLZAPFEL B., SCHULTZ L. and SAMWER K., *Phys. Rev. Lett.*, **71** (1993) 2331; URUSHIBURA A., MORITOMO Y., ARIMA T., ASAMITSU A., KIDO G. and TOKURA Y., *Phys. Rev. B*, **51** (1995) 14103; KUSTERS R. M., SINGLETON J., KEEN D. A., MCGREEVY R. and HAYES W., *Physica B*, **155** (1989) 362.
- [2] JONKER G. H. and VAN SANTEN J. H., *Physica*, **16** (1950) 337.
- [3] WOLLAN E. O. and KOEHLER W. C., *Phys. Rev.*, **100** (1955) 545.
- [4] ZENER C., *Phys. Rev.*, **81** (1951) 440; **82** (1951) 403.
- [5] DE GENNES P.-G., *Phys. Rev.*, **118** (1960) 141.
- [6] NAGAEV E. L., *Sov. Phys. Usp.*, **166** (1996) 833.
- [7] KHOMSKII D. I. and SAWATZKY G. A., *Solid State Commun.*, **102** (1997) 87.
- [8] YUNOKI S., HU J. and MALVEZZI A. L., *Phys. Rev. Lett.*, **80** (1998) 845.
- [9] KAGAN M. YU., KHOMSKII D. I. and MOSTOVOY M. V., cond-mat/9804213.
- [10] FONER S., in *Magnetism*, edited by G. T. RADO and H. SUHL, Vol. **I** (Academic Press) 1984, p. 383.
- [11] MORIYA T., in *Magnetism*, edited by G. T. RADO and H. SUHL, Vol. **I** (Academic Press) 1984, p. 85.
- [12] KITTEL CH., *Einführung in die Festkörperphysik* (Oldenburg, München) 1991, p. 528.
- [13] MOUSSA F., HENNION M., RODRIGUEZ-CARVAJAL J., MOUDDEN H., PINSARD L. and REVCOLEVSCHI A., *Phys. Rev. B*, **54** (1996) 15149.
- [14] MITSUDO S., HIRANO K., NORJIRI H., MOTOKAWA M., HIROTA K., NISHIZAWA A., KANEKO N. and ENDOH Y., *J. Magn. & Magn. Mater.*, **177-181** (1998) 877.
- [15] CINADER G., *Phys. Rev.*, **155** (1967) 453.
- [16] DZYALOSHINSKY I., *J. Phys. Chem. Solids*, **4** (1958) 241.
- [17] IVANOV V. YU., TRAVKIN V. D., MUKHIN A. A., LEBEDEV S. P., VOLKOV A. A., PIMENOV A., LOIDL A., BALBASHOV A. M. and MOZHAEV A. V., *J. Appl. Phys.*, **83** (1998) 7180.
- [18] HENNION M., MOUSSA F., RODRIGUEZ-CARVAJAL J., PINSARD L. and REVCOLEVSCHI A., *Physica B*, **234-236** (1997) 851; HENNION M., MOUSSA F., BIOTTEAU G. and RODRIGUEZ-CARVAJAL J., *Phys. Rev. Lett.*, **81** (1998) 1957; BIOTTEAU G., HENNION M., MOUSSA F., RODRIGUEZ-CARVAJAL J., PINSARD L. and REVCOLEVSCHI A., *Physica B*, **259-261** (1999) 826.
- [19] BALBASHOV A. M., KARABASHEV S. G., MUKOVSKII YA. M. and ZVERKOV S. A., *J. Cryst. Growth*, **167** (1996) 365.
- [20] MUKHIN A. A., IVANOV V. YU., TRAVKIN V. D., LEBEDEV S. P., PIMENOV A., LOIDL A. and BALBASHOV A. M., *JETP Lett.*, **68** (1998) 356; POPOV YU. F., KADOMTSEVA A. M., VOROB'EV G. P., IVANOV V. YU., MUKHIN A. A., ZVEZDIN A. K. and BALBASHOV A. M., *J. Appl. Phys.*, **83** (1998) 7160.
- [21] KOZLOV G. and VOLKOV A., in *Millimeter and Submillimeter Wave Spectroscopy of Solids*, edited by GRÜNER G. (Springer, Berlin) 1998, p. 51.
- [22] LOFLAND S. E., RAY V., KIM P. H., BHAGAT S. M., GHOSH K., GREENE R. L., KARABASHEV S. G., SHULYATEV D. A., ARSENOV A. A. and MUKOVSKII Y., *J. Phys. Condens. Matter*, **9** (1997) L633.